Choice of FACTS Device Control Inputs for Damping Interarea Oscillations

M. M. Farsangi, Y. H. Song, *Senior Member, IEEE*, and Kwang Y. Lee, *Fellow, IEEE*

***Abstract*—A method is proposed in this paper to select the input signals for both single and multiple flexible ac transmission system (FACTS) devices in small and large power systems. Different input-output controllability analyses are used to assess the most appropriate input signals (stabilizing signal) for the static var compensator (SVC), the static synchronous compensator (SSSC), and the unified power-flow controller (UPFC) for achieving good damping of interarea oscillations. The study presented in this paper is carried out on one small system with one FACTS device at a time; and one large system equipped with the SVC, the SSSC, and the UPFC.**

***Index Terms*—FACTS devices, input-output controllability analysis, input signal selection, optimal location, power system oscillation, stabilizing signal.**

I. Introduction

THE location and input signal play an important role in the ability of control devices to stabilize the interarea oscillations. In a practical power system, allocation of the devices depends on a comprehensive analysis of the steady-state stability, the transient stability, the small-signal stability and the voltage stability. Moreover, other practical factors, such as cost and installation conditions, also need to be considered.

The placing of many controllable power system devices, such as the high voltage dc (HVDC) links and the flexible ac transmission system (FACTS) devices, is based on the issues unrelated to the damping of oscillations in the system. For instance, a static var compensator (SVC) improves transmission system voltage, thereby enhancing the maximum power transfer limit; the static synchronous compensator (SSSC) control reduces the transfer impedance of a long line, enhancing the maximum power transfer limit. An additional benefit of the FACTS devices is the potential for improving system damping. The selection of appropriate stabilizing signals and effective tuning of such damping controls is an important consideration.

In recent years, numerous papers have been published to discuss and find ways to answer the question of which location and feedback signal could result in the power system stabilizer (PSS) and the FACTS devices having the maximum effect on the system. For example, static interaction measures derived from decentralized control theory such as the relative gain array (RGA) and controllability and observability have been applied to investigate both, the problems of the best location and the selection of the input signals for multiple FACTS devices [1]. Several papers also exist dealing with the combined application of controllability and observability using the singular value analysis for power system analysis [2], [3].

Reference [4] presented a detailed study on the use of a SVC for damping system oscillations. Having considered several factors including observability and controllability, it was concluded that the most suitable auxiliary input signal for the SVC for damping improvement is the locally measured transmission line-current magnitude. This signal is also used in the study carried out in [5], [6]. Other studies, however, select locally measured active power [7], [8] or generator angular speed [9]–[11] as a stabilizing signal.

Generally, two methodologies have been applied by most researchers to simultaneously determine the location and input signal for a single power system damping controller. Residue analysis is derived from modal control theory of linear time-invariant system [7], [12] and damping torque analysis [8], [9], [13]. As pointed out in [12], [14], residue analysis is equivalent to damping torque analysis. There are other techniques that do consider the effect of controls on other eigenvalues [15], but such methods are limited to considering a selected number of modes rather than determining the effect of the proposed control globally on the entire system. Once applied to a practical power system, the designed power system damping controller may cause other modes to become unstable because of the interaction with other dynamic devices.

Reference [16] adopted a frequency domain method to coordinate several SVCs in order to damp interarea oscillations in the Mexican interconnected power system, as well as to minimize the potential for adverse interaction between control loops.

Reference [17] proposed an approach to determine the number and locations of the thyristor-controlled series compensator (TCSC) in a multimachine power system. The index of optimal allocation of the controllers is the power system stability. First, the steady-state stability is considered, and then the transient stability is examined to find a robust allocation of the TCSC controller. Both small-signal and transient stability were studied in [17]. For small-signal stability system eigenvalues were used, and for transient stability the H_∞ norm was used as a performance index. Simulation results on the test system showed that one TCSC with proper controllers satisfied the small-signal stability requirements for the system, while four TCSCs were required to ensure transient stability.

Rather than on the selection of the optimal location for a FACTS device, this paper focuses on the most suitable stabilizing signal for supplementary damping control on a FACTS

Manuscript received April 30, 2003.

M. M. Farsangi is with Kerman University, Kerman, Iran.

Y. H. Song is with the Brunel Institute of Power Systems, Brunel University, Uxbridge UB8 3PH, U.K. (e-mail: Y.H.Song@brunel.ac.uk).

K. Y. Lee is with the Department of Electrical Engineering at the Pennsylvania State University, University Park, PA 16802 USA (e-mail: kwanglee@psu.edu).

Digital Object Identifier 10.1109/TPWRS.2003.820705

device for the purpose of system damping. Often the selection of the most suitable stabilizing signal is based on an observability index. In this paper in addition to the observability, other indicators are also used.

A new method is proposed in the paper to select the most responsive input signals (stabilizing signals) to the modes of oscillation for supplementary control of both single and multiple FACTS devices (or in general, for any power system damping control). The method is applicable in damping out both a single interarea oscillation mode in a small power system and multiple interarea oscillation modes in an extensively interconnected power system.

This method uses the minimum singular values (MSV), the right-half plane zeros (RHP-zeros), the relative gain array (RGA), and the Hankel singular values (HSV) as indicators to find stabilizing signals in the single-input single-output (SISO) and multi-input multi-output (MIMO) systems. In the SISO system with one FACTS device, only the criterion of RHP-zeros is used as the indicator for limiting the performance of the closed-loop system and the HSV as the indicator for controllability-observability. This is because the MSV and the RGA are useful indicators to quantify the degree of directionality [18] and the level of interaction in the MIMO systems. In the MIMO system, using multiple FACTS devices, all four indicators are utilized, which are explained in the next section.

II. Selection of Location and Input Signals for FACTS Devices

A. Minimum Singular Value (MSV)

The minimum and maximum singular values can be used to quantify the degree of directionality in the MIMO systems. Considering a MIMO system with transfer function G with n inputs and m outputs, G can be decomposed with the singular value decomposition as follows:

$$G = U\Sigma V^H \tag{1}$$

where $\Sigma = \begin{bmatrix} \Sigma_1 & 0 \\ 0 & 0 \end{bmatrix}$ is a $m \times n$ matrix and Σ_1 is defined as

$$\Sigma_1 = \begin{bmatrix} \sigma_1 & 0 & \cdots & 0 \\ 0 & \sigma_2 & \cdots & 0 \\ \vdots & \vdots & \ddots & \vdots \\ 0 & 0 & \cdots & \sigma_k \end{bmatrix}$$

in which the non-negative singular values $\sigma_1 \geq \sigma_2 \geq \cdots \sigma_i \geq \cdots \sigma_k \geq 0$ are placed diagonally in a descending order with $k = \min\{m, n\}$ and σ_i^2 is an eigenvalue of $G^H G$, where G^H is the complex conjugate transpose of G.

In (1), the output singular vectors $[u_1\ u_2\ \cdots\ u_m]$ compose the matrix $U_{m\times m}$ and the input singular vectors $[v_1\ v_2\ \cdots\ v_n]$ compose the matrix $V_{n\times n}$. The matrices U and V can be used as indicators to evaluate the strength and weakness of input-output directions.

The maximum singular value of $G\ \overline{\sigma}(G) = \sigma_{\max}(G) = \sigma_1$ shows the largest gain for any input direction. The smallest singular value of $G\ \underline{\sigma}(G) = \sigma_{\min}(G) = \sigma_k$ is a useful controllability measure showing the smallest gain for any input direction. The ratio between maximum and minimum singular values

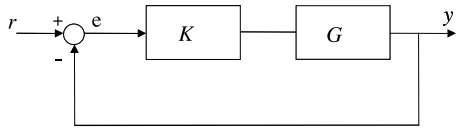

Fig. 1. Block diagram of a plant with feedback.

σ_1/σ_k indicates the degree of directionality of the system. If this ratio is big due to a small value of σ_k, it shows that the system is ill-conditioned, which indicates a large sensitivity of the system to uncertainty. To avoid the ill-conditioning, it is desired that the minimum singular value be as large as possible when selecting the input-output signal [18], [19].

B. Right-Half Plane Zeroes (RHP-Zeros)

By considering different inputs-outputs for any plant G different zeros will appear. Those inputs-outputs, which produce the RHP zeros (especially within the closed-loop bandwidth) are undesirable because of the limiting performance of the closed loop.

Considering the negative feedback system shown in Fig. 1 with plant $G = z/p$ and a constant gain controller $K = k$, the closed-loop transfer function G_c is

$$G_c = \frac{KG}{1+KG} = \frac{kz}{p+kz} = k\frac{z_{cl}}{P_{cl}}.$$

From the above closed-loop transfer function, it is obvious that the locations of zeros are unchanged, while pole locations are changed by the feedback. As the feedback gain decreases, the closed-loop poles will be moved to open-loop poles and as the feedback gain increases, the closed-loop poles will be moved from open-loop poles to open-loop zeros, which may lead to gain instability.

Thus, the selection of inputs-outputs should be carried out in a way that the closed-loop plant has a minimum number of the RHP-zeros, which are required not to lie within the closed-loop bandwidth [18].

C. Relative Gain Array (RGA)

A measure of interactions caused by decentralized control can be provided using a relative gain array (RGA). Assume u_j and y_i are, respectively, an input and an output of a multivariable plant G with m inputs and m outputs, and that y_i is controlled by u_j. The RGA is a matrix of the relative gains, and a relative gain is the ratio of two gains in two extreme cases defined as follows.

First, all other loops are open. All other input changes are zero and the gain is

$$\left(\frac{\Delta y_i}{\Delta u_j}\right)_{\Delta u_k=0,\forall k\neq j} = g_{ij} = [G]_{ij}. \tag{2}$$

Second, all other loops are closed. All other output changes are zero and the gain is

$$\left(\frac{\Delta y_i}{\Delta u_j}\right)_{\Delta y_k=0,\forall k\neq i} = \hat{g}_{ij} = \frac{1}{[G^{-1}]_{ji}} \tag{3}$$

where

$[G]_{ij}$ element of G on the ith row and jth column;

$[G^{-1}]_{ji}$ element of G^{-1} on the jth row and ith column.

The ratio of g_{ij} and $\hat{g}_{ij}$ is known as the ijth relative gain, which is defined as

$$\lambda_{ij} = \frac{g_{ij}}{\hat{g}_{ij}} = [G]_{ij}[G^{-1}]_{ji}. \tag{4}$$

All of the relative gains λ_{ij} compose the RGA, which can be expressed as

$$\Lambda = G \times (G^{-1})^T \tag{5}$$

where $\times$ denotes an element by element multiplication known as the Hadamard or the Schur product and T is the transpose operation of a matrix.

The RGA possesses the following main properties.

- It is independent of input and output scaling.
- Each row and each column sum up to 1.0, $\sum_{i=1}^{m} \lambda_{ij} = 1$.
- RGA_{ij} is independent of how other loops are paired.

The third property makes the RGA particularly attractive in making variable pairing decisions because all possible pairings can be scanned simultaneously without a prior requirement for a given pairing.

Clearly, it is desired to pair u_j and y_i so that λ_{ij} is close to 1, because this means that the gain from u_j to y_i is unaffected by closing other loops. On the other hand, a pairing corresponding to $\lambda_{ij} < 0$ is undesirable, because it means that the steady-state gain in a given loop changes sign when other loops are closed. If a pairing of an output and an input corresponds to a negative steady-state relative gain, then the closed-loop system has at least one of the following properties.

- The overall closed-loop system is unstable.
- The loop with the negative relative gain is unstable by itself.
- The closed-loop system is unstable if the loop with the negative relative gain is opened.

Based on the above explanation, the RGA (5) gives useful information to pairing inputs-outputs for a MIMO system. It is designed to pair inputs and outputs such that the diagonal elements of the RGA matrix are as close as possible to unity, which shows less interaction. Also, it is not desirable for a plant to have large RGA elements [18], [20].

The relative interaction in the decentralized control can be presented by the matrix $E = (G - \tilde{G})\tilde{G}^{-1}$ [21], [22], where matrix $\tilde{G} = diag(G_{ii})$ denotes the matrix with the diagonal elements of G. Then an important relationship for decentralized control is given by

$$\underbrace{(I + GK)}_{Overall} = \underbrace{(I + E\tilde{T})}_{\text{interactions}} \quad \underbrace{(I + \tilde{G}K)}_{individual\ loops} \tag{6}$$

where the complementary sensitivity function $\tilde{T} = \tilde{G}K(I + \tilde{G}K)^{-1}$ is the closed-loop transfer function of the diagonal system $\tilde{G}$.

Equivalently (6) can be written in terms of the sensitivity function as follows:

$$S = \tilde{S}(I + E\tilde{T})^{-1} \tag{7}$$

where $\tilde{S}$ is the sensitivity function for the diagonal system $\tilde{G}$. Note that the sensitivity functions and complementary sensitivity functions for the individual loops are collected in the diagonal matrices, that is $\tilde{S} = diag(\tilde{s}_i) = (I + \tilde{G}K)^{-1}$ and $\tilde{T} = diag(\tilde{t}_i) = \tilde{G}K(I + \tilde{G}K)^{-1}$.

Equation (7) shows that $\tilde{S}$ is not equal to the matrix of diagonal elements of S and it also depends on the interaction term $(I + E\tilde{T})^{-1}$, indicating interactions between different loops. At frequencies where the feedback is effective, $\tilde{T} \approx I$ and it can be shown that

$$(I + E\tilde{T})^{-1} \approx \tilde{G}G^{-1} = \Gamma \tag{8}$$

where $\Gamma = \{\gamma_{ij}\}$ is the performance relative gain array (PRGA), known as an indicator for interaction [18], [22]. By substituting (8) into (7), the following equation can be derived:

$$S \approx \tilde{S}\Gamma. \tag{9}$$

With this approximation, the output error e can be expressed as follows (Fig. 1):

$$e = r - y \approx \tilde{S}\Gamma r - \tilde{S}\Gamma G_d d. \tag{10}$$

Equations (9) and (10) show that Γ is important when evaluating performance with decentralized control [18], [22]. The PRGA elements larger than 1 imply there are interactions [22].

D. Hankel Singular Values (HSV)

Controllability and observability of a system play an important role in selecting input-output signals. In order to specify which combination of input-output contains more information about the system internal states, one possible approach is to evaluate observability and controllability indexes of the system.

A linear time invariant system can be defined as

$$G : \begin{cases} \dot{x} = Ax + Bu \\ y = Cx + Du \end{cases}. \tag{11}$$

Two possible ways to check that the above system is controllable are

- (A, B) is controllable if and only if matrix Φ, defined as $\Phi = [B\ AB\ A^2B \cdots A^{n-1}B]$ has full rank n, where n is the number of states.
- (A, B) is controllable if and only if the controllability Gramian matrix defined as

$$P = \int_0^\infty e^{At}BB^Te^{A^Tt}dt \tag{12}$$

is positive definite, which has full rank n. Matrix P is the solution to the following Lyapunov equation:

$$AP + PA^T + BB^T = 0. \tag{13}$$

Also, there are two possible ways to check the observability of the above system (11):

- (A, C) is observable if and only if matrix Ψ, defined as $\Psi = \begin{bmatrix} C \\ CA \\ \vdots \\ CA^{n-1} \end{bmatrix}$ has full rank n.
- (A, C) is observable if and only if the observability Gramian matrix defined as

$$Q = \int_0^\infty e^{A^Tt}CC^Te^{At}dt \tag{14}$$

has full rank n and, thus, is positive definite. Matrix Q satisfies the following Lyapunov equation:

$$A^TQ + QA + C^TC = 0. \tag{15}$$

The Hankel Singular Values (HSV) σ_i is an observability-controllability index, defined as

$$\sigma_i = \sqrt{\lambda_i(PQ)}, \quad i = 1, \ldots, n \tag{16}$$

which reflects the joint controllability and observability of the states of a system where $\lambda_i(PQ)$ is the i^{th} eigenvalue of PQ.

Thus, for choosing input and output signals, the HSV can be calculated for each combination of inputs and outputs, the candidate with the largest HSV shows better controllability and observability properties. It means that this candidate can give more information about system internal states [18].

III. Procedure of Selection of Stabilizing Signal(s) for FACTS Devices

The procedure to select stabilizing signals for supplementary controller of the FACTS devices using the MSV, the RHP-zeros, the RGA-number, and the HSV can be described as follows.

In a SISO system, using only one FACTS device, the RHP-zeros and the HSV are used as indicators to select the most responsive signal to a mode of the interarea oscillation. The procedure to carry out the selection of a proper stabilizing signal is summarized in the following steps:

- Step 1) After placing a FACTS device, choose the stabilizing signal candidates for supplementary control.
- Step 2) For each candidate, calculate the RHP-zeros. If any RHP-zeros is encountered in the frequency range of 0.1–2 Hz that is undesirable, then the corresponding candidate should be discarded.
- Step 3) Check the observability and controllability of the remaining candidates using the HSV. The candidate with the largest HSV is more preferred, which shows that the corresponding signal is more responsive to the mode of oscillation and is the final choice.

For a MIMO system using multiple FACTS devices, in addition to using the HSV and the RHP-zeros, the MSV and the RGA-number are also used to find the most responsive signals to modes of the interarea oscillation. The procedure can be described as follows:

- Step 1) Place the FACTS devices in the system. Choose the possible stabilizing signal candidate sets for supplementary control.
- Step 2) Calculate the MSV for the candidate sets in step 1. In the case of having a large number of candidate sets, a range of candidate sets with larger values of the MSV should be selected for a more detailed input-output controllability analysis.
- Step 3) Calculate the RHP-zeros for the selected candidate sets considered in step 2. Those candidate sets, which encounter the RHP-zeros, will be discarded.
- Step 4) Calculate the RGA-number for the remaining candidate sets from step 3. Candidate sets with smaller RGA-number are preferred. Few candidate sets with the RGA-number close to the achieved smallest RGA-number will be selected for the next step.
- Step 5) The observability and controllability of the selected candidate sets from step 4 will be checked using the HSV. The candidate set with the largest HSV is preferred and known as the final choice for the stabilizing signals for the supplementary controllers.

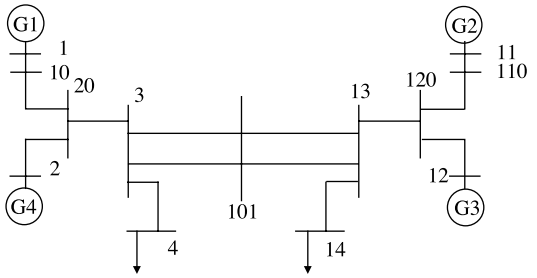

Fig. 2. Single line diagram of a two-area study system.

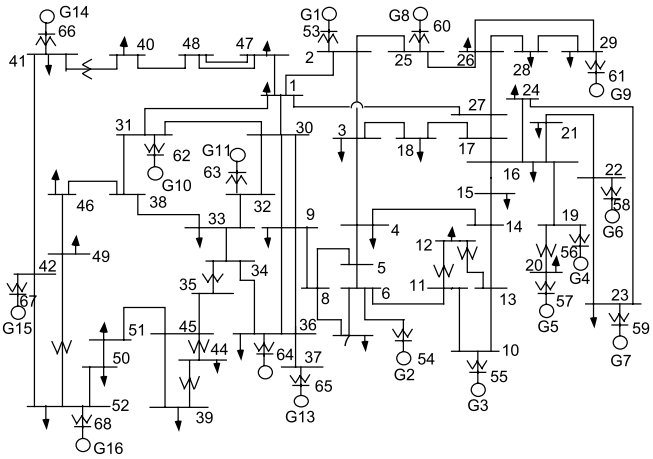

Fig. 3. Single line diagram of a five-area study system.

IV. Most Effective Stabilizing Signal(s) for the Study Systems

Two study systems, one small and one large are used in this paper. A brief description of the systems is given as follows.

Study system 1: A 2-area-4-machine system: This test system is illustrated in Fig. 2. The subtransient model for the generators, the IEEE-type DC1 and DC2 excitation system are used for machines 1 and 4, respectively, Models IEEE-type ST3 compound source rectifier exciter models is used for machine 2 and first-order simplified model for the excitation systems is used for machine 3, PSS is placed on machines 2 and 3 and the linear models for the loads are used. The system data are adopted from [23]. A three-phase fault is applied in one of the tie circuits at bus 101 between bus 101 and bus 13. The circuit is tripped after 70 ms.

Study system 2: A 5-area-16-machine system: The system shown in Fig. 3, consists of 16 machines and 68 buses. This is a reduced order model of the "old" New England (NE) New York (NY) interconnected system [24]. The system does not represent the current New York-New England interconnected system. The first

TABLE I
ENCOUNTERED RHP-ZEROS FOR THE 4 STABILIZING SIGNAL CANDIDATES

Candidate No.	Stabilizing signal candidate	RHP-zeros of System with SVC	RHP-zeros of System with SSSC	RHP-zeros of System with UPFC
1	$I_{20\text{-}3}$	Yes	Yes	Yes
2	$P_{20\text{-}3}$	No	No	No
3	$I_{120\text{-}13}$	Yes	No	No
4	$P_{120\text{-}13}$	No	No	No

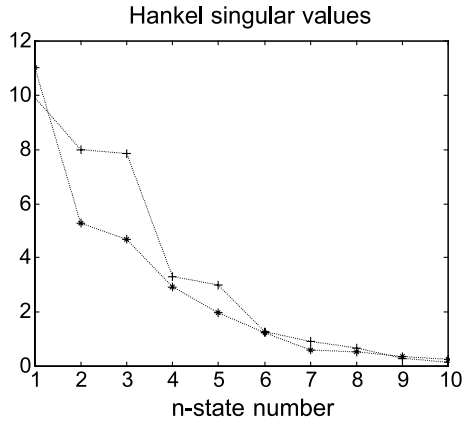

Fig. 4. HSV of the candidates 2 and 4 for the system 1 equipped with SVC: plus-dotted line: candidate 2; star-dotted line: candidate 4.

nine machines are the simple representation of the New England system generation. Machines 10 to 13 represent the New York power system. The last three machines are the dynamic equivalents of the three large neighboring areas interconnected to the New York power system. The subtransient reactance model for the generators, the first-order simplified model for the excitation systems, and the linear models for the loads and ac network are used. Also, the system data are adopted from [24]. A three-phase fault is applied in bus 1 between bus 1 and bus 2. The circuit is tripped after 70 ms.

A. Study System 1 Equipped With the SVC, SSSC, and UPFC

For this system, the SVC is to be located at bus 101, the SSSC at line 101-13, and the UPFC at bus 101 and line 101-13. Since only one FACTS device is to be located in this system at a time, the most effective signal is chosen based on the RHP-zeros and HSV. Once the FACTS devices are placed in the system, the choices for the stabilizing signal could be as I_{20-3}; P_{20-3}; I_{120-13}; or P_{120-13} [25].

First, the RHP-zeros for the above candidates for the SVC, the SSSC, and the UPFC are calculated. Table I shows whether the candidates encountered the RHP-zeros or not. For the SVC as shown in Table I, only the candidates 1 and 3 encountered the RHP-zeros. This analysis leaves us with the candidates 2 and 4 for a further consideration by the HSV. As illustrated in Fig. 4, statistically the HSV for the candidate 2 is larger than the HSV for the candidate 4. In other words, candidate 2 contains more information about the system internal states than output 4. Therefore, candidate 2 is more preferable than candidate 4 and is selected as the final choice.

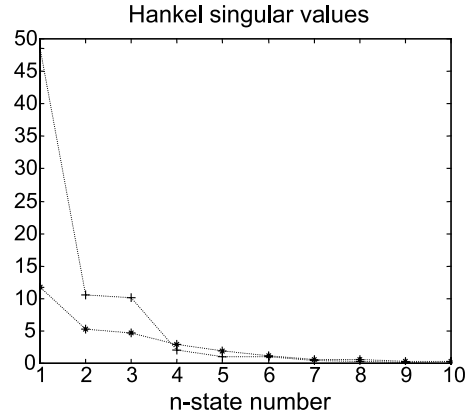

Fig. 5. HSV of the candidates 2 and 3 for the system 1 equipped with SVC: plus-dotted line: candidate 3; star-dotted line: candidate 2.

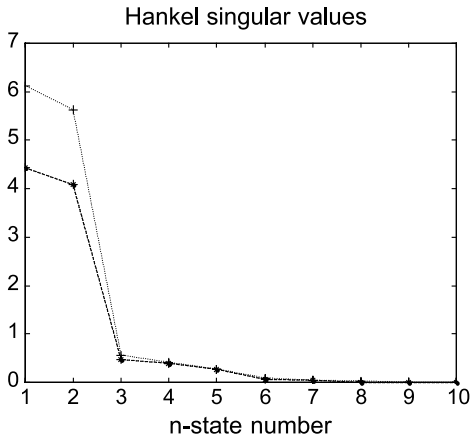

Fig. 6. HSV of candidates 2, 3, and 4 for the system 1 equipped with SSSC: plus-dotted line: candidate 3; star-dotted line: candidates 2 and 4.

Before carrying on the signal selection procedure for the SSSC and UPFC, an extra piece of analysis is carried out here for the SVC to show that a decision made according to the observability alone is inadequate. To show this, the observabilities of two candidates (candidates 2 and 3) are compared as shown in Fig. 5. As illustrated in this figure, the HSV for candidate 3 is larger than the HSV of candidates 2; however, candidates 3 has been discarded because it produces RHP-zeros. This analysis shows that the other factors of input-output controllability analysis must be taken into consideration before making decision based on the observability.

For the SSSC and the UPFC, the same procedure is applied to select stabilizing signals. As can be seen from Table I, only candidate 1 produces the RHP-zeros. The HSV for the remaining candidates (2, 3, and 4) for the SSSC and the UPFC are performed and the results are shown in Figs. 6 and 7, respectively. As illustrated in these figures, the achieved HSV for the three candidates are close to each other, which shows that any of them can be selected as the final choice. Candidate 3 is selected as the final choice for stabilizing signal for both the SSSC and UPFC.

B. Study System 2 Equipped With SVC, SSSC, and UPFC

For the study system, 2 UPFC is placed at bus 8 and line 8–9, and SSSC and SVC are placed at line 40–48 and bus 7, respectively. While the FACTS devices are placed into the power

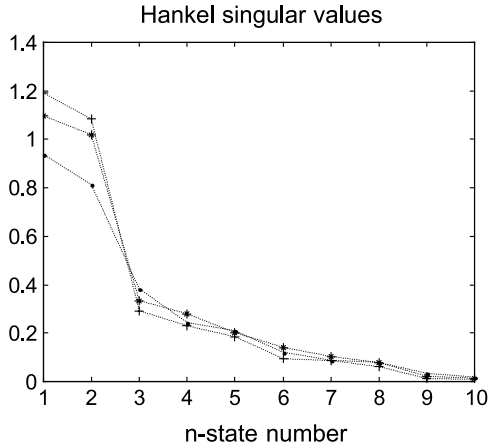

Fig. 7. HSV of candidates 2, 3, and 4 for the system 1 equipped with UPFC: plus-dotted line: candidate 3; star-dotted line: candidate 2; dot-dotted line: candidate 4.

system, the choices of the candidates for the feedback signals could be as follows:

For the SVC, the possible candidates are $[\mathrm{I}_{6-7};\ \mathrm{I}_{7-8};\ \mathrm{I}_{9-36};\ \mathrm{I}_{9-30};\ \mathrm{P}_{6-7};\ \mathrm{P}_{7-8};\ \mathrm{P}_{9-36};\ \mathrm{P}_{9-30}]$.
For the UPFC, the possible candidates are $[\mathrm{I}_{5-8};\ \mathrm{I}_{9-36};\ \mathrm{I}_{9-30};\ \mathrm{P}_{5-8};\ \mathrm{P}_{9-36};\ \mathrm{P}_{9-30}]$.
For the SSSC, the possible candidates are $[\mathrm{I}_{40-41};\ \mathrm{I}_{40-48};\ \mathrm{P}_{40-41};\ \mathrm{P}_{40-48}]$.

With the above choices of feedback signals, it is desired to select one signal for the SVC, one signal for the SSSC, and one signal for the UPFC. Thus, the numbers of possibilities are $8 \times 6 \times 4 = 192$.

The 192 candidate sets are analyzed with detailed input-output controllability analysis using the MSV, the RHP-zeros, the RGA-number, and the HSV. At each step, some of the candidates are eliminated.

The MSV for all 192 candidate sets are calculated. The achieved largest MSV value is 2.5079 and the achieved smallest one is 0.0007. Candidate sets with very small MSV compared to the candidate set with maximum MSV (2.5079) cause ill-conditioning, which should be eliminated. Candidate sets with the MSV close to 2.5079 are more preferable. However, the candidate sets with the MSV value in a wider range between 0.0630 and 2.5079 are selected (39 candidates) for the next step.

At this step, the RHP-zeros for these 39 candidate sets are calculated. Since it is required to control the plant between 0.1–2 Hz, the RHP-zeros close to these values cause problems and, therefore, are avoided. Among the 39 candidate sets, only 20 candidates do not encounter the RHP-zeros as listed in Table II and the other 19 candidates are eliminated. This analysis leaves us with the 20 selected candidate sets for further consideration by the RGA-number.

The RGA for the candidate sets having the MSV larger than 0.15 (12 candidates as bolded in Table II) are checked for the frequency of interest. The candidates with the smallest RGA are the best. Among these 12 candidates, candidate sets 11–13 and 15 in Table II have smaller RGA as shown in Fig. 8. These four candidates are chosen for the next step. The final decision is made using the HSV analysis.

TABLE II
MSV FOR THE CANDIDATE SETS OF THE STUDY SYSTEM 2

Set No.	Candidates	MSV
1	I7-8, I40-41, I9-30	0.0630
2	I7-8, I48-47, I9-36	0.1228
3	I7-8, P41-40, I9-36	0.1418
4	I7-8, P41-40, I9-30	0.0690
5	I7-8, I47-48, I5-8	**0.2009**
6	I7-8, P41-40, I5-8	**0.1982**
7	I7-8, I48-47, P9-36	**0.2422**
8	I7-8, P41-40, P9-36	**0.1973**
9	I6-7, I48-47, I9-36	0.1103
10	I6-7, P41-40, I9-36	0.1247
11	I6-7, I47-48, I5-8	**2.5079**
12	I6-7, P40-41, I5-8	**2.1999**
13	I6-7, P47-48, I5-8	**0.2140**
14	I6-7, I48-47, P9-36	**0.1950**
15	I6-7, P41-40, P9-36	**0.1589**
16	I6-7, P41-40, P5-8	**1.9185**
17	I6-7, P47-48, P5-8	**0.2079**
18	P9-36, I47-48, I5-8	0.1437
19	P9-36, I40-41, I5-8	0.115
20	P6-7, I40-48, I5-8	**0.1573**

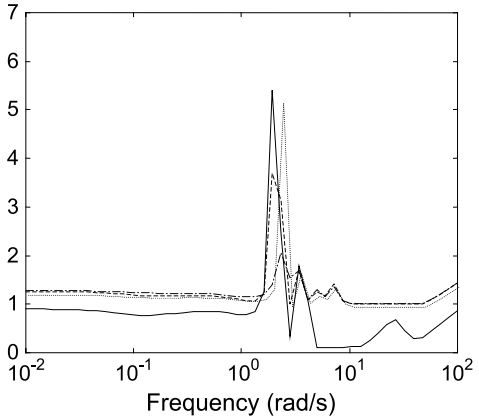

Fig. 8. RGA plot of candidates 11, 12, 13, and 15 for the system 2: solid line: candidate 15; dashed line: candidate 13; dotted line: candidate 12; dashed-dotted line: candidate 11.

It is found that candidate set 15 has the largest HSV among the candidate sets 11–13 as illustrated in Figs. 9–11. These figures indicate that the candidate set 15 has better state controllability and observability properties. Therefore, the candidate set 15 is more preferable for control purposes and hence is selected as the final choice. These stabilizing signals are used to design the controllers for the UPFC, the SSSC, and the SVC in the later stage of this study.

C. Performance Evaluation in the Study System 1

The purpose of this and the following sections is to show that the selected signals are effective in controlling the modes of oscillation. For this, the study system 1 is equipped with a SVC. A supplementary controller is designed for the SVC using the H_∞ mixed-sensitivity method (the method is explained in [26]).

A three-phase fault is applied in one of the tie circuits at bus 101. An eigenvalue analysis is carried out to evaluate the damping ratios for prefault and postfault conditions. The entries in Table III display the damping ratios and interarea modes of

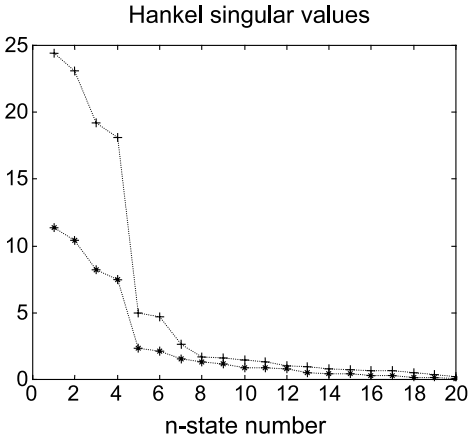

Fig. 9. HSV of the candidate sets 11 and 15: plus-dotted line: candidate 15; star-dotted line: candidate 11.

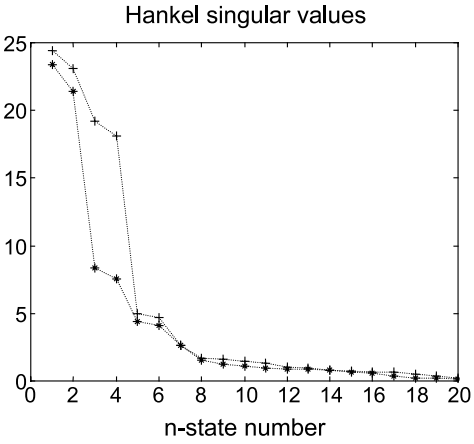

Fig. 10. HSV of the candidate sets 12 and 15: plus-dotted line: candidate 15; star-dotted line: candidate 12.

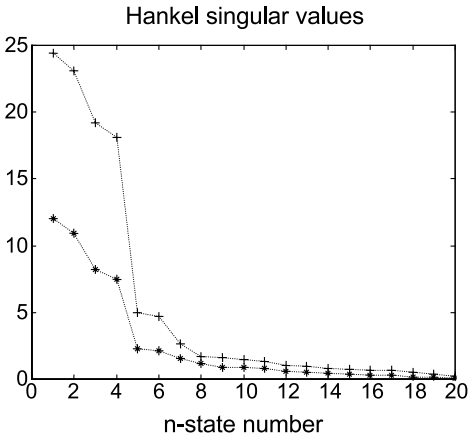

Fig. 11. HSV of the candidate sets 13 and 15: plus-dotted line: candidate 15; star-dotted line: candidate 13.

the system with and without the SVC and when the system is equipped with the SVC and the supplementary controller.

Also, a nonlinear time-domain simulation has been carried out for the study system 1 equipped with the SVC as shown in Fig. 12.

Table III and Fig. 12 show that the location of SVC with the selected signal for the supplementary controller is effective in controlling the mode of oscillation.

TABLE III
EFFECTS OF SVC ON EIGENVALUES AND DAMPING RATIOS OF THE INTERAREA MODE

System Condition	Pre-fault		Pre-fault	
	Inter-area Mode	ζ	Inter-area Mode	ζ
Without SVC	-0.180±3.504i	0.051	-0.021±2.817i	0.007
With SVC	-0.258±3.744i	0.068	-0.086±2.90i	0.029
SVC with supplementary Controller	-0.315±3.761i	0.083	-0.286±3.751i	0.076

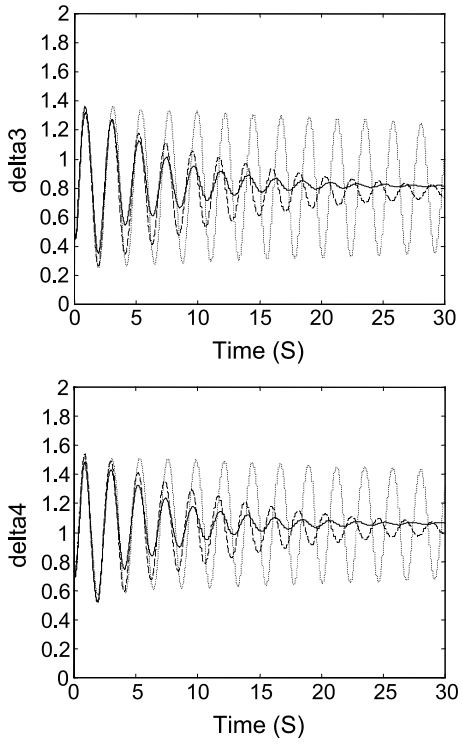

Fig. 12. Response of generators to a three-phase fault: dotted line: without SVC; dashed line: with SVC; solid line: with SVC and the supplementary controller.

D. Performance Evaluation in the Study System 2

In order to determine the interaction between loops 1 (SVC), 2 (SSSC), and 3 (UPFC), the PRGA for the study system is plotted as shown in Fig. 13.

PRGA elements larger than 1 imply that there are adverse interactions [18] and this figure shows that there are interactions from loop 1 into loop 2 (G_{21}) and into loop 3 (G_{31}).

A three-phase fault at bus 1 is assumed in the tie-lines between bus 1 and bus 2. An eigenvalue analysis is carried out to evaluate the damping ratios for postfault conditions. The entries in Table IV display the interarea mode and damping ratios in the open loop for the study system 2. It can be seen from this table that after clearing the fault, one eigenvalue will be positive and the system is expected to become unstable through growing oscillations.

By placing the FACTS devices, the unstable mode disappears. By applying supplementary controllers, damping will

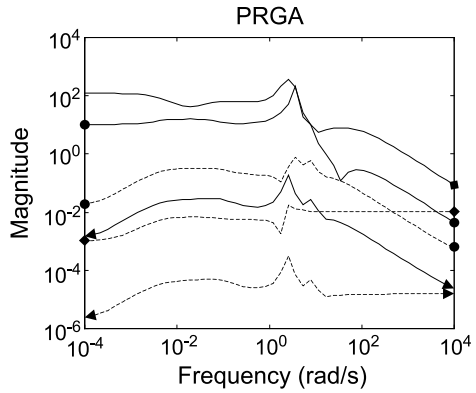

Fig. 13. Elements of PRGA: **Lines ended by square**: dashed line: G_{32}; solid line: G_{31}; **Lines ended by circle**: dashed line: G_{23}; solid line: G_{21}; **Lines ended by arrow**: dashed line: G_{13}; solid line: G_{12}.

TABLE IV
EFFECTS OF FACTS ON EIGENVALUES AND DAMPING RATIOS OF THE INTERAREA MODES (STUDY SYSTEM 2)

Mode No.	Without FACTS Devices		With FACTS Devices	
	Inter-area Mode	ζ	Inter-area Mode	ζ
1	0.0116±1.812i	-0.006	-0.1043±1.909i	0.054
2	-0.0511±2.919i	0.017	-0.0584±3.026i	0.019
3	-0.1427±3.165i	0.045	-0.1657±3.173i	0.052
4	-0.2446±4.946i	0.049	0.2489±4.938i	0.050

TABLE V
EFFECTS OF CLOSED-LOOP ON DAMPING RATIOS OF THE INTERAREA MODES (STUDY SYSTEM 2)

Closed-loop	Mode 1	Mode 2	Mode 3	Mode 4
Pre-fault	0.094004	0.085436	0.093633	0.07045
Post-fault	0.091890	0.095240	0.092090	0.07020

be improved further. Table V shows the damping ratio of the closed-loop system with the supplementary controllers for the study system 2. In Table V, the location of modes changed slightly from prefault to postfault conditions.

To verify the performance of the controllers in the face of the system nonlinearity, a nonlinear simulation is performed.

Tables IV and V and Fig. 14 show that the locations of the FACTS devices with the selected signals for the supplementary controller are responsive to the modes of oscillation.

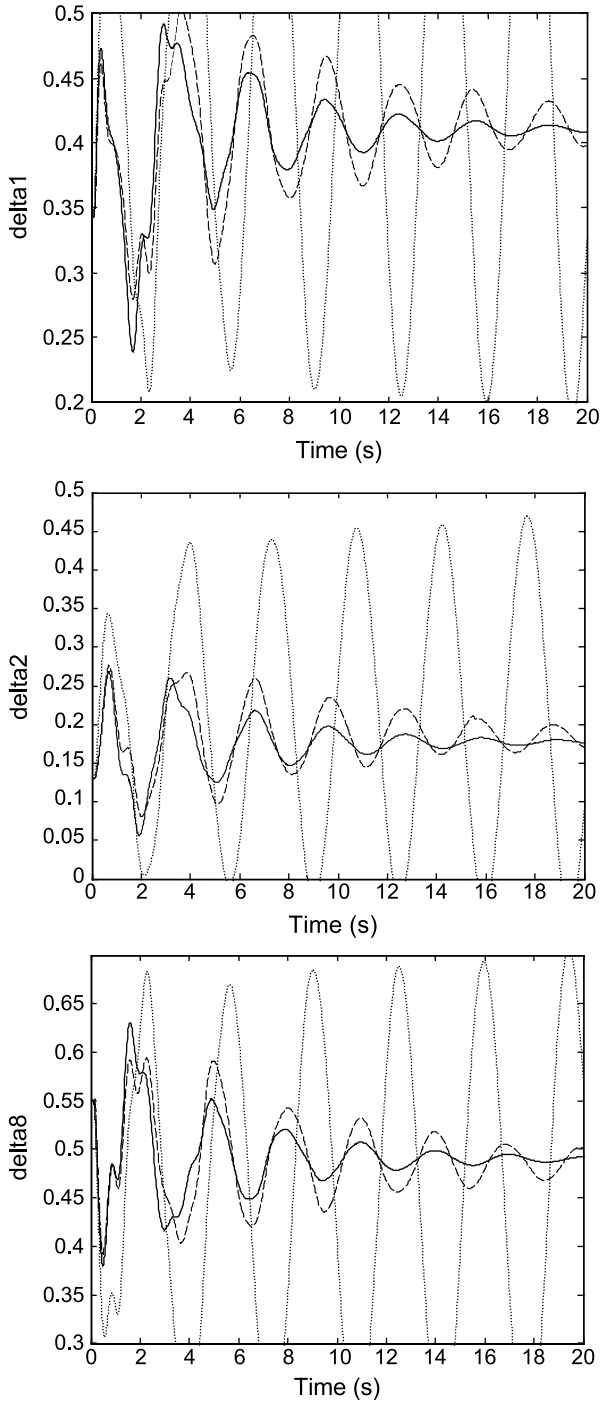

Fig. 14. Dynamic response of the system following a three-phase fault at bus 1 in the study system 2: dotted line: without FACTS devices; dashed line: FACTS devices without controllers; solid line: FACTS devices with supplementary controllers.

V. CONCLUSION

In this paper, the importance of identifying effective stabilizing signals for the FACTS devices in a power system is highlighted. It is concluded that the method of controllability and observability alone as an analytical tool is not adequate to identify the most effective feedback signals. The final selection should be carried out in a more detailed input-output controllability analysis. In SISO systems, this task can be done using the RHP-zeros and the HSV indicators. For MIMO systems, in addition to the RHP-zeros and the HSV, other indicators, the MSV and the RGA-number, are used.

With the chosen signals for SISO and MIMO systems, the corresponding supplementary controllers are designed. The results show that the selected signals are responsive to interarea modes.

REFERENCES

[1] P. Zhang, A. R. Messina, A. Coonick, and B. J. Cory, "Selection of locations and input signals for multiple SVC damping controllers in large scale power systems," in *Proc. IEEE Power Eng. Soc. Winter Meeting*, 1998, Paper IEEE-0-7803-4403-0, pp. 667–670.

[2] A. O. Ekwue, H. B. Wan, D. T. Y. Cheng, and Y. H. Song, "Singular value decomposition method for voltage stability analysis on the National Grid system (NGC)," *Int. J. Elect. Power Energy Syst.*, vol. 21, no. 6, pp. 425–432, 1999.

[3] A. M. A. Hamdan, "An investigation of the significance of singular value decomposition in power system dynamics," *Int. J. Elect. Power Energy Syst.*, vol. 21, no. 6, pp. 417–424, 1999.

[4] E. V. Larsen and J. H. Chow, SVC control design concepts for system dynamic performance, in IEEE Special Publications: Application of Static VAR Systems for System Dynamic Performance, pp. 36–53, 1987.

[5] Q. Zhao and J. Jiang, "Robust SVC controller design for improving power system damping," *IEEE Trans. Energy Conversion*, vol. 10, pp. 201–209, June 1995.

[6] ——, "A TCSC damping controller design using robust control theory," *Elect. Power Energy Syst.*, vol. 20, no. 1, pp. 25–33, 1998.

[7] N. Martins and L. T. G. Lima, "Determination of suitable locations for power system stabilizers and Static VAR Compensators for damping electromechanical oscillations in large scale power systems," *IEEE Trans. Power Syst.*, vol. 5, pp. 1455–1469, Nov. 1990.

[8] P. Pourbeik and M. J. Gibbard, "Damping and synchronizing torques induced on generators by FACTS stabilizers in multimachine power systems," *IEEE Trans. Power Syst.*, vol. 11, pp. 1920–1925, Nov. 1996.

[9] S. E. M. De Oliveira, "Synchronizing and damping torque coefficients and power system steady-state stability as affected by static VAR compensators," *IEEE Trans. Power Syst.*, vol. 9, pp. 109–119, Feb. 1994.

[10] S. Lee and C. C. Liu, "An output feedback static var controller for the damping of generator oscillations," *Elect. Power Syst. Res.*, vol. 25, no. 1, pp. 9–16, 1994.

[11] E. Z. Zhou, "Application of static var compensators to increase power system damping," *IEEE Trans. Power Syst.*, vol. 8, pp. 655–661, May 1993.

[12] H. F. Wang, F. J. Swift, and M. Li, "Selection of installing locations and feedback signals of FACTS-based stabilisers in multimachine power systems by reduced-order modal analysis," *Proc. Inst. Elect. Eng., Gen. Transm. Dist.*, vol. 144, no. 3, pp. 263–269, May 1997.

[13] B. T. Ooi, M. Kazerani, R. Marceau, Z. Wolanski, F. D. Galiana, D. McGillis, and G. Joos, "Mid-point siting of FACTS devices in transmission lines," *IEEE Trans. Power App. Syst.*, vol. 100, pp. 3933–3939, Aug. 1997.

[14] H. F. Wang, F. J. Swift, and M. Li, "Indices for selecting the best location of PSS's or FACTS-based stabilisers in multimachine power systems: a comparative study," *Proc. Inst. Elect. Eng., Gen. Transm. Dist.*, vol. 144, no. 2, pp. 155–159, Mar. 1997.

[15] P. Pourbeik and M. J. Gibbard, "Simultaneous coordination of power system stabilizers and FACTS device stabilizers in a multimachine power system for enhancing dynamic performance," *IEEE Trans. Power Syst.*, vol. 13, pp. 473–479, May 1998.

[16] A. R. Messina, S. D. Olguin, S. C. A. Rivera, and D. Ruiz-Vega, "Analytical investigation of large scale use of Static VAr Compensation to aid damping of inter-area oscillations," in *Proc. 7th Int. Conf. AC-DC Power Transm.*, London, U.K., 2001, pp. 187–192.

[17] M. Ishimaru, G. Shirai, K. Y. Lee, and R. Yokoyama, "Allocation and design of robust TCSC controllers based on power system stability index," in *Proc. IEEE Power Eng. Soc. Winter Meeting*, vol. 1, 2002, pp. 573–578.

[18] S. Skogestad and I. Postethwaite, *Multivariable Feedback Control, Analysis and Design*. New York: Wiley, 1996.

[19] K. Zhou, J. C. Dole, and K. Glover, *Robust and Optimal Control*. Englewood Cliffs, NJ: Prentice-Hall, 1996.

[20] M. Hovd and S. Skogestad, "Simple frequency-dependent tools for control system analysis, structure selection and design," *Automatica*, vol. 28, no. 5, pp. 989–996, Sept. 1992.

[21] P. Grosdidier and M. Morari, "Interaction measures for systems under decentralised control," *Automatica*, vol. 22, no. 3, pp. 309–319, May 1986.

[22] M. Hovd and S. Skogestad, "Sequential design of decentralised controller," *Automatica*, vol. 30, no. 10, pp. 1601–1607, 1994.

[23] G. Rogers, *Power System Oscillations*. Norwell, MA: Kluwer, 2000.

[24] J. H. Chow, Ed., *Time Scale Modeling of Dynamic Networks With Applications to Power Systems*. Berlin, Germany: Springer-Verlag, 1982.

[25] P. Kundur, *Power System Stability and Control*. New York: McGraw-Hill, 1994.

[26] M. M. Farsangi and Y. H. Song, "Sequential decentralised control of FACTS devices in large power systems," in *Proc. 7th Int. Conf. AC-DC Power Transm.*, London, U.K., Nov. 2001, pp. 268–273.

M. M. Farsangi received the first degree from Kerman University, Kerman, Iran, in 1999, and the Ph.D. degree in electrical engineering from Brunel Institute of Power Systems, Brunel University, Uxbridge, U.K., in 2003.

Currently, she is with Kerman University. Her interests include power system control and stability.

Y. H. Song (SM'94) is a Professor of Electrical Energy Systems at Brunel Institute of Power Systems, Brunel University, Uxbridge, U.K., where he has been since 1997. His research interests include power system optimization, control, economics, FACTS, and intelligent system applications.

He is a fellow of the IEE and a chartered electrical engineer in the U.K. In 2002, he was awarded the D.Sc. degree by Brunel University for his significant contributions to power system knowledge and research.

Kwang Y. Lee (F'01) received the B.S. degree in electrical engineering from Seoul National University, Korea, in 1964, the M.S. degree in electrical engineering from North Dakota State University, Fargo, in 1968, and the Ph.D. degree in System Science from Michigan State University, East Lansing, in 1971.

Currently, he is Professor of Electrical Engineering and Director of Power Systems Control Laboratory at Pennsylvania State University, University Park. He has also been with Michigan State, Oregon State University, Corvallis; and the University of Houston. His research interests include power system control, operation, planning, and intelligent system applications to power systems. He is Associate Editor of IEEE TRANSACTIONS ON NEURAL NETWORKS, and Editor of IEEE TRANSACTIONS ON ENERGY CONVERSION.